



## Original Article

# Therapeutic potential of exosomes derived from human endometrial mesenchymal stem cells for heart tissue regeneration after myocardial infarction

Masoumeh Sepehri <sup>a</sup>, Shahram Rabbani <sup>b</sup>, Jafar Ai <sup>a</sup>, Naghmeh Bahrami <sup>a, c</sup>,  
 Hossein Ghanbari <sup>d</sup>, Mojdeh Salehi Namini <sup>a</sup>, Majid Sharifi <sup>e</sup>, Fatemeh Kouchakzadeh <sup>f</sup>,  
 Mohsen Abedini Esfahlani <sup>a</sup>, Somayeh Ebrahimi-Barough <sup>a, \*</sup>

<sup>a</sup> Department of Tissue Engineering, School of Advanced Technologies in Medicine, Tehran University of Medical Sciences, Tehran, Iran

<sup>b</sup> Research Center for Advanced Technologies in Cardiovascular Medicine, Cardiovascular Diseases Research Institute, Tehran University of Medical Sciences, Tehran, Iran

<sup>c</sup> Craniomaxillofacial Research Center, Tehran University of Medical Sciences, Tehran, Iran

<sup>d</sup> Department of Medical Nanotechnology, School of Advanced Technologies in Medicine, University of Medical Sciences, Tehran, Iran

<sup>e</sup> Department of Tissue Engineering, School of Medicine, Shahrood University of Medical Sciences, Shahrood, Iran

<sup>f</sup> Department of Histology, School of Paramedical, Shahid Sadoughi University of Medical Sciences, Yazd, Iran

## ARTICLE INFO

## Article history:

Received 2 December 2024

Received in revised form

26 December 2024

Accepted 10 January 2025

## Keywords:

Human endometrium mesenchymal stem cells

Myocardial infarction

Heart regeneration

Exosomes

Angiogenesis

## ABSTRACT

Myocardial infarction (MI) is the most common cardiovascular disease (CVD) and the leading cause of mortality worldwide. Recent advancements have identified human endometrial mesenchymal stem cells (hEnMSCs) as a promising candidate for heart regeneration, however, challenges associated with cell-based therapies have shifted focus toward cell-free treatments (CFTs), such as exosome therapy, which show considerable promise for myocardial tissue regeneration. MI was induced in male Wistar rats by occluding the left anterior descending (LAD) coronary artery. The hEnMSCs-derived exosomes (hEnMSCs-EXOs) were encapsulated in injectable fibrin gel inside the cardiac tissue. The encapsulated hEnMSC-EXOs were administered, and their effects on myocardial regeneration, angiogenesis, and heart function were monitored for 30 days post-MI. The treatments were evaluated through histological analysis, echocardiographic parameters of left ventricular internal dimension at end-diastole (LVIDD) and end-systole (LVID), left ventricular end-diastole volume (LVEDV), left ventricular end-systole volume (LVESV), and left ventricular ejection fraction (LVEF) and molecular studies. Histological findings demonstrated significant fibrosis and left ventricular remodeling following MI. Treatment with fibrin gel-encapsulated hEnMSCs-EXOs substantially reduced fibrosis, enhanced angiogenesis, and prevented heart remodeling, leading to improved cardiac function. Notably, 30 days after encapsulated hEnMSCs-EXOs were delivered corresponded with a less inflammatory microenvironment, supporting cardiomyocyte retention in ischemic tissue. This study highlights the potential of encapsulated hEnMSCs-EXOs in fibrin gel as a novel therapeutic strategy for ischemic myocardium repair post-MI. The findings underscore the importance of biomaterials in advancing stem cell-based therapies and lay a foundation for clinical applications to mitigate heart injury following MI.

© 2025 The Author(s). Published by Elsevier BV on behalf of The Japanese Society for Regenerative Medicine. This is an open access article under the CC BY-NC-ND license (<http://creativecommons.org/licenses/by-nc-nd/4.0/>).

**Abbreviations:** CVDs, Cardiovascular diseases; MI, Myocardial infarction; CTE, Cardiac tissue engineering; SCT, Stem cell therapy; MSCs, Mesenchymal stem cells; CFTs, Cell-free treatments; hEnMSCs, Human Endometrial MSCs; hEnMSCs-EXO, hEnMSCs-derived exosomes; LVIDD, left ventricular internal dimension at end-diastole; LVIDS, left ventricular internal dimension at end-systole; LVEDV, Left ventricular end-diastole volume; LVESV, Left ventricular end-systole volume; LVEF, Left Ventricular Ejection Fraction.

\* Corresponding author. Department of Tissue Engineering, School of Advanced Technologies in Medicine, University of Medical Sciences, Tehran, Iran.

E-mail address: [ebrahimi\\_s@sina.tums.ac.ir](mailto:ebrahimi_s@sina.tums.ac.ir) (S. Ebrahimi-Barough).

Peer review under responsibility of the Japanese Society for Regenerative Medicine.

<https://doi.org/10.1016/j.reth.2025.01.007>

2352-3204/© 2025 The Author(s). Published by Elsevier BV on behalf of The Japanese Society for Regenerative Medicine. This is an open access article under the CC BY-NC-ND license (<http://creativecommons.org/licenses/by-nc-nd/4.0/>).

## 1. Introduction

Cardiovascular diseases (CVDs) are among the leading causes of mortality globally, with the World Health Organization (WHO) predicting that by 2030, CVD-related deaths will exceed 22.2 million [1]. Myocardial infarction (MI), a common and severe complication of CVD, results from the narrowing and blockage of coronary arteries, leading to ischemia, irreversible myocardial necrosis, and the formation of fibrotic scar tissue. MI causes significant damage to the heart, resulting in left ventricular deformation and remodeling, electrophysiological dysfunction, and impaired cardiac contractility [2,3]. Due to the limited regenerative capacity of mature cardiomyocytes, extensive myocardial cell death during ischemia often leads to heart failure [4].

Current therapeutic approaches for MI have shown clinical success, including methods to restore blood flow, pharmacological treatments to reduce cardiac remodeling and surgical interventions. However, these treatments primarily focus on managing symptoms rather than regenerating damaged heart tissue, ultimately only delaying the progression from MI to heart failure. The limitations of existing therapies and the shortage of donor organs for heart transplantation have led to the exploration of cardiac tissue engineering (CTE) as a promising therapeutic alternative for myocardial regeneration [5].

Stem cell therapy (SCT) has emerged as a potential strategy for cardiomyocyte replacement following MI. The use of adult stem cells, such as bone marrow-derived mesenchymal stem cells (BM-MSCs), skeletal myoblasts, and cardiac progenitor cells (CPCs), has been explored in cardiac cell therapies since the early 2000s [6–9]. Among these, mesenchymal stem cells (MSCs) from various sources, are considered primary candidates for regenerating damaged myocardium due to their multipotency and ability to improve heart function [10–12]. Recent studies have also highlighted the promising regenerative potential of human endometrial mesenchymal stem cells (hEnMSCs), which are characterized by high self-renewal rates and potent angiogenic properties. These cells are immune privileged and can be accessed non-invasively, making them an attractive candidate for regenerative therapies [13–15]. Angiogenesis, the process of new blood vessel formation, is a key therapeutic property of MSCs and MSCs-derived exosomes. Exosomes secreted by stem cells have shown promise in myocardial repair, exerting similar effects on endothelial and myocardial cells as the parent stem cells themselves. Notably, hEnMSCs have demonstrated superior angiogenic properties compared to BM-MSCs, and preclinical studies have confirmed their beneficial effects on heart failure and critical limb ischemia [16–19]. Exosomes, a type of extracellular vesicle (EV) with a lipid bilayer membrane ranging in size from 30 to 150 nm, contains a variety of bioactive molecules, including cell adhesion proteins, heat shock proteins, tetraspanins, coding and non-coding RNAs, cytosolic molecules, metabolites, and lipids [20–22]. These components contribute to intracellular communication, targeted homing, angiogenesis, and the transfer of antigens to dendritic cells (DCs). Compared to their parent cells, exosomes not only retain the same bioactive molecules for cell receptor communication but also lack tumorigenic potential and immune response due to the absence of self-replicating entities [23–25]. Several studies have demonstrated that exosomes derived from various mesenchymal stem cells (MSCs) can promote cardiac tissue regeneration after myocardial infarction (MI) [26–28]. These exosomes facilitate the delivery of endogenous cargos to myocardial tissue, fibroblasts, and endothelial cells, stimulating cardiomyocyte proliferation and angiogenesis. However, their retention in the myocardium is limited, typically lasting less than 3 h, due to washout from the heart's blood flow [29,30]. Recent advances in delivery platforms, such as injectable hydrogels, have

been developed to enhance the retention and therapeutic efficacy of exosomes by improving their stability and prolonging their release at the ischemic site [31,32]. Fibrin gel, a biocompatible and FDA-approved hydrogel, has shown promise in encapsulating exosomes, thereby stabilizing their contents and enhancing their therapeutic potential for myocardial regeneration [33,34]. Despite the encouraging results from preclinical studies, the clinical translation of exosome therapy remains hindered by challenges such as short half-life, rapid clearance by the immune system, and off-target effects. However, exosome-based therapies, with their low immunogenicity and minimal ethical concerns, hold significant potential as a novel treatment for myocardial infarction and other cardiovascular conditions.

This project aims to explore the therapeutic potential of exosomes derived from hEnMSCs (hEnMSCs-EXOs) for heart tissue engineering. Using an *in vivo* rat model of MI, we can assess the effects of hEnMSCs-EXOs in promoting myocardial regeneration, to advance this novel approach toward clinical applications.

## 2. Materials and methods

### 2.1. Ethics

All animal experiments were approved by the Ethics Committee of the Tehran University of Medical Sciences (Ethical Approval No. IR. TUMS.AMIRALAM.REC.1402.041) following institutional and international guidelines. Rats were treated according to guidelines for the "Care and Use of Laboratory Animals" [35]. A total of 25 male Wistar rats (8–10 weeks old) with an average weight of  $300 \pm 50$  g were enrolled in this study. Rats were kept in standard cages with a constant humidity of 50–60 % at 25 °C and 12: 12 light-dark cycle. Animals were allowed to access chewing foods and drinking water *ad libitum*.

### 2.2. *In vitro* analyses

#### 2.2.1. Isolation of human endometrial MSCs (hEnMSCs)

Isolation of hEnMSCs was performed according to the described method by Mohamadi et al. [36]. In Brief, endometrial tissue was obtained with informed consent from patients who went to the Imam Khomeini Hospital (Tehran, Iran) for infertility treatment, healthy women aged 20–35 years in the secretory phase of their menstrual cycle provided endometrial biopsies. All experiments and protocols of this study were approved by the Ethics Committee of Tehran University of Medical Science. The endometrial tissues were placed in Hank's medium supplemented with 1 % Pen-Strep and 1 mg/ml amphotericin B, upon arrival at the cell culture laboratory. Subsequently, the specimens were washed with warm Hank's medium with the same supplements. Then the tissues were transferred into sterile 15 ml Falcon tubes filled with 1 mg/ml collagenase I and incubated at 37 °C for 30–45 min. Followed by, a pre-warmed sterile complete medium (DMEM/F12 + FBS10 %, 1 % Pen-Strep) was added to neutralize the collagenase I. To separate the glandular epithelial components, the suspension was passed by cell strainers of 70  $\mu$ m Falcon cell strainer once and 40  $\mu$ m Falcon cell strainer, respectively. The cells that passed through the filter were centrifuged at  $300 \times g$  for 10 min. Then, Ficoll (Sigma, USA) was used to remove the mononuclear cells. The supernatant was discarded, and the cell pellet was resuspended in 1 ml of pre-warmed plating medium (DMEM-F12 with 15 % FBS, 1 % Pen-Strep, 1 % glutamine, and 1 mg/ml amphotericin B). This cell suspension was added to culture flasks along with an additional 2.5 ml of plating medium and incubated for 24 h. The following day, an extra 3 ml of plating medium was added, and the cells were cultured for a week in a cell incubator. Once the cells reached 90 %

confluence, they were harvested for the first passage. Finally, the differentiation characterization and surface markers of these cells (hEnMSCs) and then utilized for the animal study were studied after passage 3.

### 2.2.2. Characterization of human endometrial MSCs (hEnMSCs)

The expression of hEnMSCs markers was assayed by using flow cytometry (Abcam Co., Cambridge, UK). Briefly, the suspension of hEnMSC (passage 3) was added to each vial containing antibodies of anti-(CD105, CD90, CD146, CD34, and CD31) and then incubated for 1 h (4 °C). Finally, cells were fixed in 100 ml paraformaldehyde (1 %), and the statistical record was analyzed by the Becton Dickinson device (BD Biosciences CA, USA) and flowing software 2.5.1. Notably, data were calculated and expressed as mean  $\pm$  SD,  $n = 3$ .

To differentiate hEnMSCs into adipose and osteoblast cells, passages 3 of hEnMSCs (at the concentration of  $2 \times 10^4$  cells/well) were cultured in DMEM-F12 supplemented with 10 % FBS. When the cells were 70–80 % confluent, the DMEM-F12 medium was replaced with a differentiation medium of adipogenic and or osteogenic. The cells were treated with the mentioned medium for 3 weeks. Finally, the hEnMSCs after fixation by 4 % PFA, were stained by the Oil red O method to evaluate differentiation into adipose cells and by Alizarin red S staining protocol to confirm osteogenic differentiation.

### 2.2.3. Isolation and characterization of hEnMSC-derived exosomes

Human Enriched Mesenchymal Stem Cells (hEnMSCs) at passage three were cultured in DMEM/F12 supplemented with 10 % fetal bovine serum (FBS) and 1 % penicillin-streptomycin, under standard conditions of 37 °C and 5 % CO<sub>2</sub>. Once the cells reached over 80 % confluence, they were transferred to a serum-free culture medium for 48 h. Exosomes were isolated from the hEnMSCs culture supernatant when cell confluence exceeded 70 %. The supernatant was first centrifuged at 300g for 10 min to remove cells, followed by a second centrifugation at 2000g for 10 min and a final centrifugation at 10,000g for 30 min to eliminate dead cells, cell debris, and larger particles. Exosomal pellets were subsequently obtained using an exosome isolation kit (Exocib C) and resuspended in phosphate-buffered saline (PBS) for further characterization.

To determine the concentration of the isolated exosomes, a Bradford assay was performed. Different concentrations of bovine serum albumin (BSA) were prepared, with 10  $\mu$ L of each concentration added to a 6-well plate containing 200  $\mu$ L of Bradford reagent. Absorbance was measured at a wavelength of 595 nm, allowing for the quantification of exosomes via a standard curve. The size distribution of exosomes was analyzed using dynamic light scattering (DLS) with a Zetasizer Nano ZS, where 50  $\mu$ L of exosome suspension was diluted in 950  $\mu$ L of PBS. Measurements were conducted using standard parameters (absorption: 0.01; refraction: 1.38; temperature: 25 °C).

Morphological analysis and particle size assessment of the exosomes were conducted using scanning electron microscopy (SEM, KYKY-Digital SEM M3200). A 10  $\mu$ L aliquot of the exosome suspension was deposited on a glass slide and allowed to dry for 4 h, after which samples were fixed, dehydrated, and coated with gold for SEM imaging at an accelerating voltage of 25.0 kV. Additionally, Western blotting was performed to assess the presence of the exosomal marker protein CD63. Total exosomal proteins were extracted using RIPA buffer, separated by 12 % sodium dodecyl sulfate-polyacrylamide gel electrophoresis (SDS-PAGE), and transferred to a nitrocellulose membrane. The membrane was blocked with a solution containing 5 % milk and 0.05 % Tween-20 in PBS for 24 h at room temperature, followed by incubation with primary anti-CD63 monoclonal antibody for 2.5 h. After rinsing three times with PBS, the membrane was incubated with secondary

horseradish peroxidase (HRP)-conjugated antibody for 2 h, washed twice with PBS, and bands were visualized using a chemiluminescent detection system.

### 2.3. In vivo analyses

#### 2.3.1. Animal experimental design: Animal pre-surgery care, echocardiography, and ECG

The acclimatization period was done 2 weeks before surgery. During this period, clinical examinations were performed to evaluate the animal's health before the start of the surgery. Food and water were available to the animals ad libitum. Then, rats were randomly divided into 5 groups (5 in each) as follows: Sham, Control (MI group receiving no treatment), MI group treatment with encapsulated hEnMSCs-EXOs in fibrin gel for injection, MI group treatment with hEnMSCs-EXOs for injection, MI group treatment with fibrin gel for injection.

With the help of echocardiographic parameters, the structural condition or contractile disorder of the heart in all the animal groups studied, before the operation, one day after the operation, and creating the MI model, as well as conducting a follow-up after 1 and 30 days of surgery. Echocardiographic parameters are: LVIDD: left ventricular internal dimension at end-diastole, LVIDS: left ventricular internal dimension at end-systole, LVEDV: Left ventricular end-diastole volume, LVESV: Left ventricular end-systolic volume, LVEF: Left Ventricular Ejection Fraction [37].

#### 2.3.2. Induction of experimental model of MI in rats

The most common rat model of MI is by occluding the left anterior descending coronary artery (LAD). After identifying the LAD it was occluded 4 mm from the origin under the left auricle. ST elevation was seen in ECG and approved induction of MI. Air was removed from the chest cavity before it was closed by hyperventilation of the lungs. MI was induced in 20 rats, and post-MI evaluation of echocardiographic parameters and histological studies were performed 30 days later [38,39].

#### 2.3.3. hEnMSCs-derived exosomes encapsulation in fibrin gel

To facilitate the application of hEnMSCs-derived exosomes (hEnMSCs-EXOs) in heart surgery, a series of myocardial infarction (MI) animal models were used to evaluate their delivery via fibrin gel. For this procedure, a suspension of 100  $\mu$ L hEnMSCs-EXOs was prepared in a 15 ml Falcon tube, wrapped in aluminum foil to protect from light. To this, 3 mg of fibrinogen powder (Sigma) was dissolved in 1 ml of culture medium, and the solution was supplemented with 100  $\mu$ L of hEnMSCs-EXOs, providing a final concentration of 100  $\mu$ g/ $\mu$ L. In addition, 20  $\mu$ L of thrombin (100 units/mL) (Sigma) and 3.25 mM calcium chloride were added to each sample. At the time of surgery, the fibrinogen-exosome mixture was combined with thrombin by adding 300  $\mu$ L of the suspension to each thrombin-containing microtube. The resulting mixture was then drawn into an insulin syringe and immediately injected into three points surrounding the MI zone in each animal model.

In another experimental group, MI animal models were treated with only hEnMSCs-EXOs (without fibrin gel). For this group, 100  $\mu$ L hEnMSCs-EXOs were prepared in a suspension, and 300  $\mu$ L of this suspension was drawn into an insulin syringe. The hEnMSCs-EXOs suspension was then injected directly into three points surrounding the MI zone during surgery. For a third group, MI animal models were treated with fibrin gel alone. In this case, 3 mg of fibrinogen powder (Sigma) was dissolved in a culture medium and mixed with 20  $\mu$ L of thrombin (100 units/mL), following the same procedure for preparation and injection as described for the fibrin-exosome group. 300  $\mu$ L of the fibrinogen-thrombin suspension was drawn into an insulin syringe and injected into three points surrounding the MI zone.

### 2.3.4. Implantation of exosomes by injection into the MI area

To evaluate the ability of hEnMSCs-EXOs and encapsulated hEnMSCs-EXOs in fibrin gel to induce angiogenesis in the MI model rat heart, after anesthesia, it was done using 20 male Wistar rats weighing 300–350 g and aged 7–8 weeks. During the operation, the surgeon used a clean sterile gown, mask, and gloves. Using sterile surgical instruments is the best way to prevent infections related to surgery. The rat should be weighed to adjust the dose of anesthetic. Injectable anesthetics were injected into rats through the intramuscular route as a single dose. Rats were anesthetized by intraperitoneal injection of ketamine (Alfasan™, The Netherlands; 50 Mg/g1000 body weight) and medetomidine (Alfasan™, The Netherlands; 1 Mg/g1000 body weight). The chest was opened through thoracotomy and after inducing the MI model in the manner described above and confirming it with ECG, in the next step, using a 30-gauge insulin syringe, 300  $\mu$ L, with a dose of 1  $\mu$ g/ $\mu$ L of hEnMSC-EXO and encapsulated hEnMSC-EXOs in fibrin gel was injected into two of the study groups in 3 points around the area of MI in the heart, and the incisions were closed with sutures.

### 2.3.5. Histological evaluations after injections

At 30 days after injection, the animals were sacrificed. Then, by making an incision in the chest heart was exposed. The gross morphology of the tissues was observed using a stereo microscope (SMZ 1000, Japan) to examine wall thickness in the left ventricle around the MI area. Tissue samples were fixed and placed in paraffin molds and cut into 3  $\mu$ m thick pieces for hematoxylin-eosin (H&E) staining and Masson trichrome staining to evaluate wall thickness in the left ventricle in rats for quantitative analysis of infarct size. The images obtained from H&E and Masson trichrome staining were taken by an AxioCam camera on AxioPlan microscope (Carl Zeiss GmbH, DE) [38].

### 2.3.6. Measurement of wall thickness and infarct size

All histological sections were examined with a Nikon Eclipse E800 microscope using a 1x objective. Images were captured with a Retiga CCD camera with the use of Openlab software (Improvision, Lexington, MA). ImageJ 1.34 software was used to measure wall thickness, infarct size, and LV area [38].

- A) Wall Thickness: LV wall thicknesses were assessed microscopically using an objective micrometer, with average thickness reported as means  $\pm$  SD in mm.
- B) Infarct Area: The length of the infarct area was determined using the average ratio of endocardial infarct length to total endocardial length and epicardial infarct length to total endocardial length.
- C) LV Areas: LV area was calculated by measuring the left ventricular circumferential length.
- D) Infarct Size (%): Infarct size (%) was computed by dividing the total infarct areas by the total LV areas across all sections and multiplying by 100.

### 2.3.7. Immunohistochemistry (IHC)

For immunohistochemical (IHC) staining, the tissues were usually fixed with formalin for 48 h and embedded in paraffin. Then, sections with a thickness of 3  $\mu$ m were cut and placed on slides coated with silane and dried for 120 min at room temperature. Parts were dewaxed in clear xylene instead of tissue. Then they were rehydrated through serial dilution of ethanol and washed in PBS for 5 min using a hot water bath with a staining container containing sodium citrate buffer. When the temperature reached 100  $^{\circ}$ C, the sections were washed in PBS at least 3 times for 5 min and then in the same way with Triton X-1000.3 %. The samples were incubated in a blocking

buffer of 10 % normal goat serum for at least 1 h. Then, endothelial marker CD31 primary antibody was added and the sections were kept overnight at 4  $^{\circ}$ C. Sections were washed in 0.1 M PBS for 5 min at least 4 times and a secondary antibody was added for 2 h at 37  $^{\circ}$ C. Then the samples were washed 4 times in 0.1 M PBS. The prepared slides were observed and examined under an inverted microscope. Staining with hematoxylin and eosin was performed and the sections were dehydrated and placed on slides. The glass slides were randomly arranged and examined using an optical microscope and the average number of blood vessels was determined. For data evaluation, 5 sections of each scaffold and 4 images per section were examined [39].

### 2.4. Statistical analyses

All quantitative experiments were presented as mean  $\pm$  standard deviation (SD) using at least 3 independent biological replicates. The results were analyzed by one-way ANOVA using SPSS version 16.0 software. If the treatments were significant, pairwise comparisons were performed using Tukey's test. A value of  $p \leq 0.05$  % was considered as a significant level.

## 3. Results

### 3.1. Determination of hEnMSCs and hEnMSCs-EXOs characterization

Based on the results of flow cytometric analysis, the standardized culture of hEnMSCs has led to the expression of surface markers of MSCs and endometrial following the serial passage (Fig. 1. A). Accordingly, CD90 and CD105 demonstrated a higher expression level more than 99 %. The CD146 was also expressed on the surface of hEnMSCs, at higher levels than 86 %. Notably, the expression of endothelial and hematopoietic markers CD31 and CD34 was obtained lower than 3 % (i.e. 2.86 % and 1.30 % respectively) (Fig. 1. B).

Moreover, the analyses of the cellular morphology by phase contrast microscopy confirmed the same fibroblast-like and spindle-shaped morphology for the hEnMSCs (Fig. 1. A. a). hEnMSCs differentiation into osteoblast cells in the induction medium containing dexamethasone was also confirmed by the Alizarin red S staining protocol. Accordingly, the good color of the cells indicates calcium deposition in bone cells, while the control sample is not colored due to the absence of calcium (Fig. 1. A. b). Also, after treating with the induction medium which contains dexamethasone, IBMX (3-isobutyl-1-methylxanthine) for 2 weeks, the staining was carried out with Oil red O solution to confirm hEnMSCs differentiation into adipose cells. As observed in Fig. 1. A. c, the intracellular fat vacuoles are colored red.

Exosomes were isolated from hEnMSCs, and their concentration was determined using the Bradford assay along with a standard curve, revealing a concentration of 100 mg/ml (Fig. 1. C). In contrast, dynamic light scattering (DLS) analysis yielded a mean diameter of 60 nm (Fig. 1. D), which may be attributed to the aggregation of exosomes in the aqueous medium during the analysis. Scanning electron microscopy (SEM) analysis further confirmed that the hEnMSCs-EXOs have a spherical shape (Fig. 1. E), verifying their structure the results of the Western blot assay also confirmed the presence of hEnMSCs-EXOs via CD9, CD63, and CD81 (Fig. 1. F).

### 3.2. Animal study

#### 3.2.1. Confirmation of MI induction in rats

In the gross scope, blanching and cyanosis of the left ventricle anterior wall were evident (Fig. 2. A). Along with these changes,

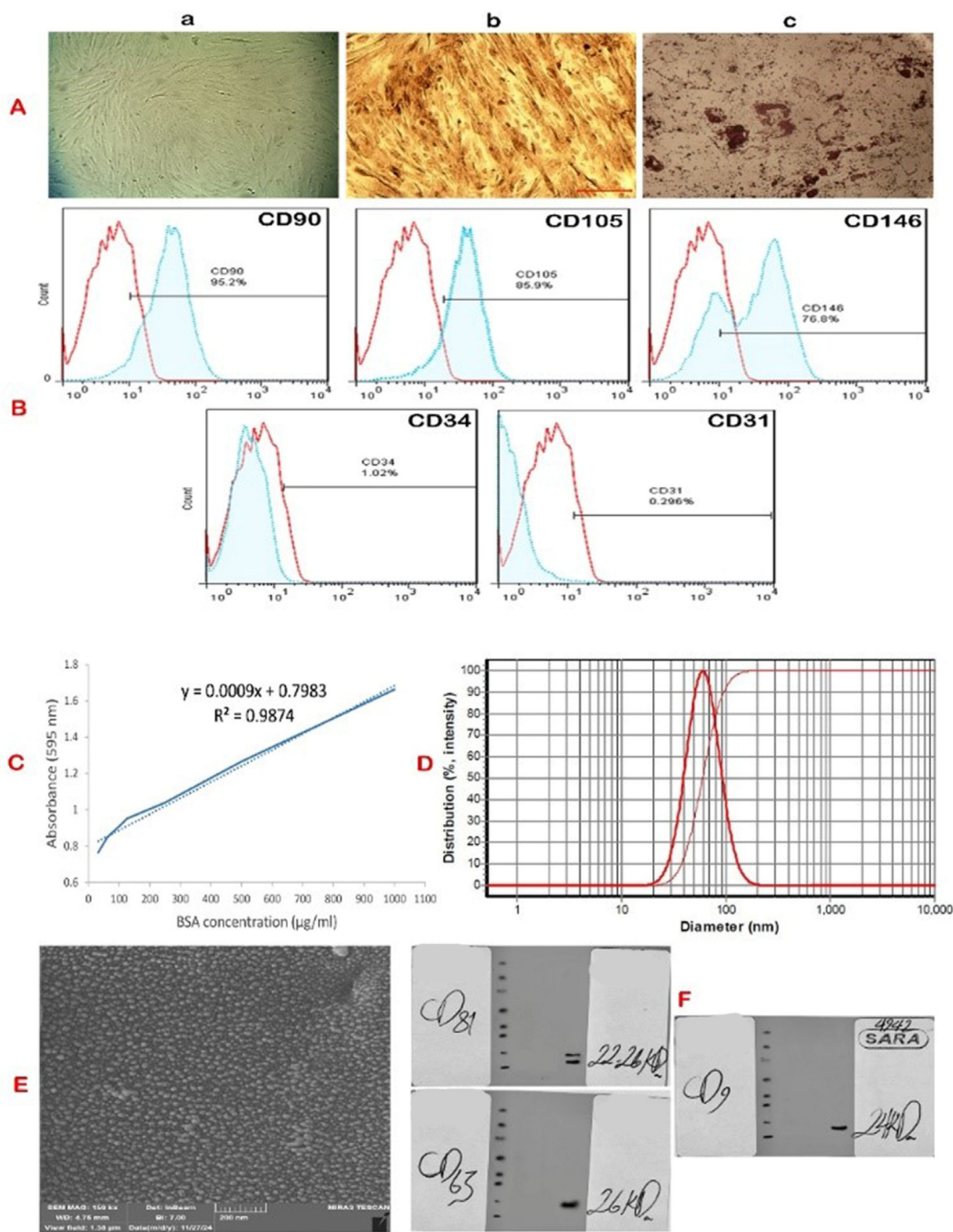


**Fig. 1.** The hEnMSCs and hEnMSCs-derived exosomes (hEnMSCs-EXOs) isolation and characterization. A) Phase contrast photomicrograph of hEnMSCs cultured in the third passage (a) and differentiated cells after 21 days of induction into osteoblast (b) and adipocyte cells (c). The cells usually appeared elongated and spindle-shaped with round nuclei. Scale bar: 100 μm. Microphotographs of isolated hEnMSCs after 21 days culture in osteogenic and adipogenic induction media stained with alizarin red and oil red o staining. (scale bar is 50 μm). B) Flow cytometric analysis of isolated hEnMSCs for mesenchymal stem cell markers (CD90, CD105, and CD146), hematopoietic marker (CD34), and endothelial marker (CD31). The isolated cells are positive for CD90, CD105, and CD146 and are negative for CD31, and CD34. C) Bradford analysis of hEnMSCs-EXOs. D) Dynamic light scattering (DLS) of hEnMSCs-EXOs. E) Image of the isolated hEnMSCs-EXOs using SEM. F) Illustration of exosome markers such as CD9, CD 63, CD81, and cytochrome C expression as a negative marker by Western blot examination.

swelling of the atrium also occurred upon ligation of the LAD coronary artery. An electrocardiogram (ECG) profile was recorded to assess ST-segment elevation before and after LAD coronary artery ligation (Fig. 2. B). Data showed a significant ST arch elevation after LAD coronary artery ligation. These features indicate the efficiency of our protocol in the induction of an experimental rat model of MI.

### 3.2.2. Encapsulated hEnMSC-EXOs in fibrin gel promoted MI healing

A total of 25 histological samples (3 histological sections for each sample) were analyzed in the current study. On day 30 post-injection, the histological sections were blindly evaluated, scored, and reported (Fig. 3) for infarct size, infarct wall thickness, and the percentage of viable myocardium in the risk area. Harris

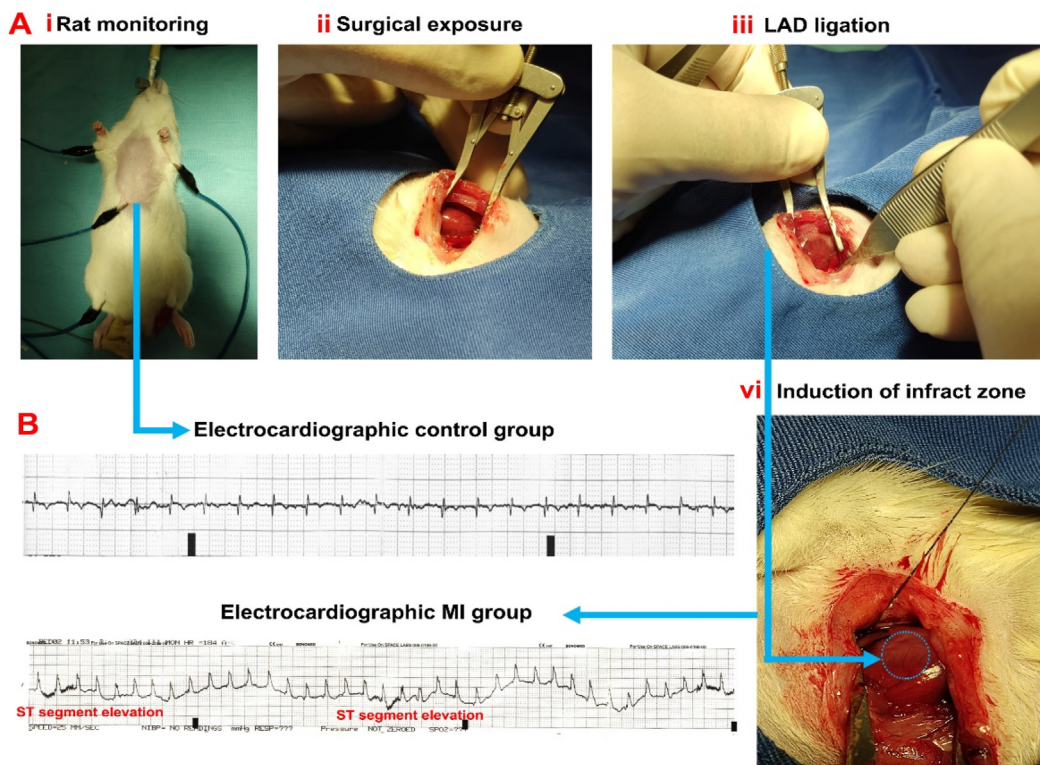


**Fig. 2.** LAD coronary artery ligation via left thoracotomy. Following LAD coronary artery ligation, the cyanotic changes can be evident at the anterior surface of the left ventricle (A). ECG analysis revealed the elevation of the ST arch in the MI group compared to the control rats (B).

hematoxylin-eosin (H&E) staining showed all treatment groups significantly higher mean histological scores than that of the control group on days 30 posttreatment. The hEnMSCs-EXOs group significantly showed higher histological scores than nontreated MI ( $p < 0.001$ ) and shame groups ( $p < 0.001$ ). In addition, the infarct (fibrosis) size in the hEnMSCs-EXOs group on day 30 post-treatment, the highest histological score was detected in the hEnMSCs-EXOs group compared with shame ( $P < 0.05$ ) and MI ( $p < 0.001$ ) groups respectively.

Masson's Trichrome (MT) staining also confirmed the histological variations in different groups. New angiogenesis is detectable by Masson trichrome staining.

### 3.2.3. Therapeutic effects of encapsulated hEnMSCs-EXOs in vivo

To validate the therapeutic effects of EXOS in vivo, a rat model of MI was created by permanently ligating the left anterior descending (LAD) artery [40]. We randomized the rats into 5 groups ( $n = 5$ ), including healthy controls (Sham), MI injury controls, and MI injured rats that were injected with encapsulated hEnMSCs-EXOs, hEnMSCs-EXOs only, and fibrin gel only.

All treatments were performed right after the MI. Cardiac function parameters were assessed immediately post-MI as the baseline and then 24 h and 30 days post-MI as the endpoint through echocardiography, including left ventricular internal diameter end-diastole (LVIDD), left ventricular internal diameter end-systole (LVIDS), left ventricular end-diastole volume (LVEDV), left ventricular end-systole volume (LVESV), and left ventricular ejection fraction (LVEF) (Fig. 4 A-E). Compared to the sham group, all MI injured rats at the baseline showed a similar level of decline on LVEF due to an elevated LVIDS and LVESV measurement. These results indicated that an equal degree of MI injury was successfully created in these animal groups, which induced weakened heart

contractility on the left ventricle myocardium (Fig. 4. B, D, and F). Thirty days after treatment, echocardiography showed that animals receiving encapsulated hEnMSCs-EXOs had the highest LVEF (Fig. 4. E). Although LVEF was also preserved in encapsulated hEnMSCs-EXOs-injected animals, the treatment efficacy was lower than that from encapsulated hEnMSCs-EXOs. We reason that the high treatment efficacy of encapsulated hEnMSCs-EXOs was largely related to an increased in situ exosome retention. H & E and Masson's trichrome staining of all hearts showed that the encapsulated hEnMSCs-EXOs heart presented a smaller infarct size, thicker left ventricular wall, and more viable cardiac tissue in the risk region (Fig. 2. B–E) when compared to other treatment groups. Altogether, these results suggested that encapsulated hEnMSCs-EXOs effectively enhanced cardiac function by reducing the infarct size, thickening the left ventricular wall, and increasing the viable cardiac tissue in the risk region.

### 3.2.4. Potential mechanisms underlying encapsulated hEnMSCs-EXOs treatment

Blood reperfusion is crucial for the repair and protection of tissue injured by myocardial infarction (MI). To investigate the potential mechanisms underlying the therapeutic effects of encapsulated hEnMSCs-EXOs, we assessed angiogenesis in the peripheral region of the MI tissue. The expression of the endothelial cell marker CD31 was compared across all treatment groups (Fig. 5). Immunohistochemistry (IHC) analysis revealed significantly higher CD31 expression in the hearts treated with encapsulated hEnMSCs-EXOs compared to the other treatment groups. This suggests that encapsulated hEnMSCs-EXOs promote angiogenesis and improve blood flow in the MI peripheral region. In summary, encapsulated hEnMSCs-EXOs enhanced cardiomyocyte proliferation and supported angiogenesis in the injured hearts, contributing to tissue repair and recovery.

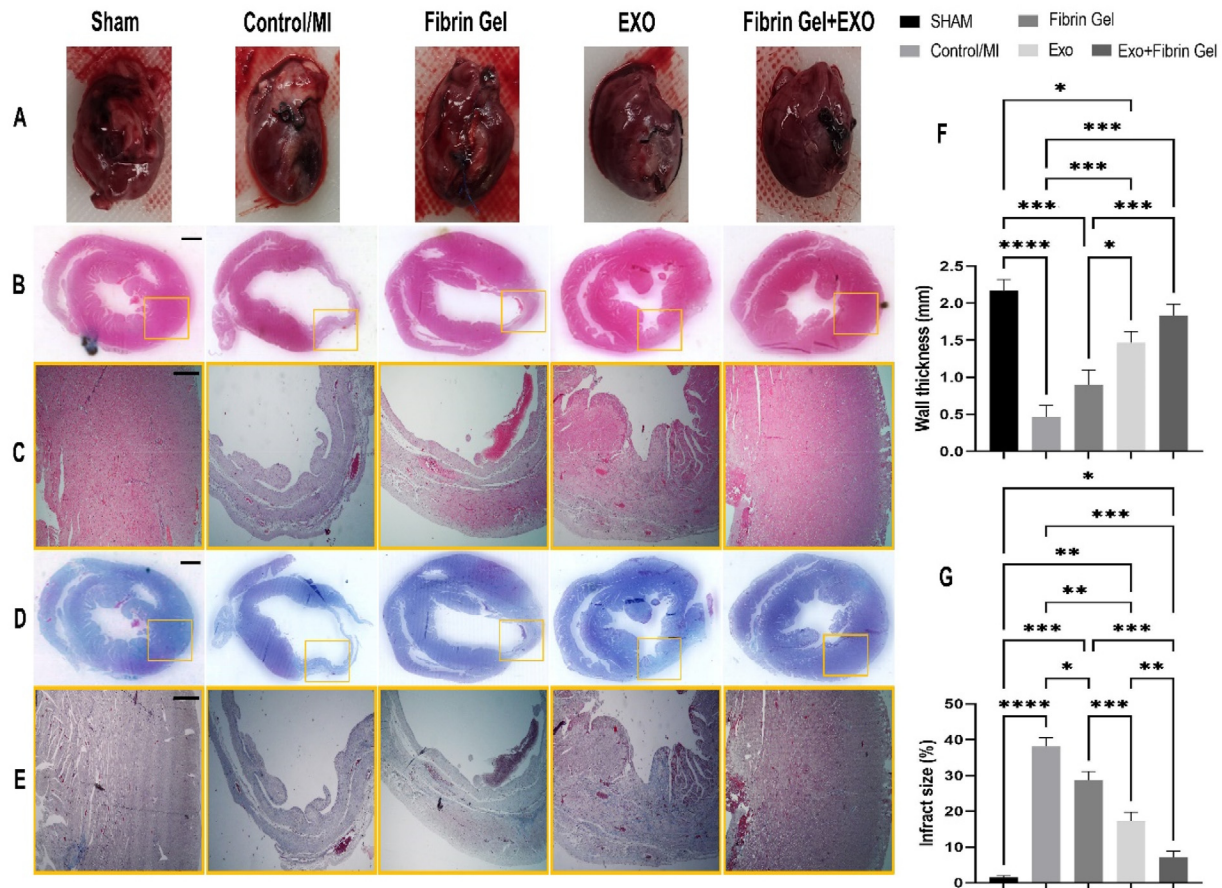


**Fig. 3.** Evaluation of cardiac remodeling in the infarcted myocardium using H & E and Masson's trichrome stainings (A–E). Hearts harvested from different groups, healthy controls (Sham), MI injury controls, and MI injured rats that were injected with encapsulated hEnMSCs-EXOs with fibrin gel (fibrin gel + EXO), hEnMSCs-EXOs only (EXO), fibrin gel only (A). H & E staining in microscopic structures from different groups (scale bar is 1 mm) (B). H & E staining in microscopic structures from different groups (scale bar is 100  $\mu$ m) (C). Masson's trichrome staining in microscopic structures from different groups (scale bar is 1 mm) (D). Masson's trichrome staining in microscopic structures from different groups (scale bar is 100  $\mu$ m) (E). Data showed the increase in anterior wall thickness in the left ventricle in rats that received encapsulated hEnMSCs-EXOs in fibrin gel, hEnMSCs-EXOs, and fibrin gel, compared to the MI group ( $p < 0.05$ ) (F). Despite the reduction of infarct zone in treatment groups (yellow dotted line), these changes were not statistically significant after 30 days (G). One-way ANOVA with Tukey post hoc analysis. ( $n = 5$ ). \*\*\*\* $p < 0.0001$ . Wall thickness in rats' treatment with encapsulated hEnMSCs-EXOs in fibrin gel reduces scar size and increases viable myocardium. (A) Representative Masson's trichrome staining images. Higher magnification pictures are shown in red dashed outline boxes. Morphometric parameters including infarct size, infarct wall thickness, and the percentage of viable myocardium in the risk area were determined with the ImageJ software, ( $n = 5$ ). All error bars are means  $\pm$  SD. The differences between samples were compared through one-way ANOVA followed by the post hoc Bonferroni test. \* Indicates  $P < 0.05$ ; \*\* indicates  $P < 0.01$ ; \*\*\* indicates  $P < 0.001$ ; \*\*\*\* indicates  $P < 0.0001$ .

Despite the important impact shown by different types of stem cells for recovery of cardiac function after MI, the low absorption and survival of transplanted cells have been a major issue. Delivery of cell-free components, such as stem cells derived-exosomes, has been shown to increase cardiomyocytes viability and myocardium regeneration. However, exosome therapy lacks the ability to promote cardiomyocyte proliferation. Moreover, exosome therapy has a short effective lifetime and mild efficacy due to limited retention in the myocardium [40–42]. Preconditioned cardiac progenitor cells (CPCs) using MSCs-derived exosomes and then transplanted the pretreated CSCs into the heart in rats MI model that the pretreatment of CSCs with exosomes had a superior effectiveness in decreasing myocardium fibrosis and improved heart function. Ong et al. [43] combined exosomes derived from endothelial cells (ECs-EXO) with CPCs and then delivered into MI mice. They demonstrated that CPCs are capable of uptaking ECs-EXO in 12 h after injection, which could confer increased tolerance to the co-transplanted CPCs at day 7.

Based on previous studies, hEnMSCs-derived exosomes carry a wide range of functional proteins, mRNAs, and miRNAs which could serve as a potential cell-free therapeutic for cardiac repair. It

seems that hEnMSCs-EXOs can promote the regeneration of myocardial tissue and lead to the control of targeted cell signaling pathways. In this field, the reports indicated that the use of hEnMSCs-EXOs can activate the cascades of BMP/Smad, Wnt/b-catenin, and PI3K/AKT, resulting in angiogenesis, and subsequently reducing of fibrosis and myocardial regeneration [44–46]. Generally, the microscopic findings (H & E, Masson trichrome staining, and IHC) demonstrate that myocardial regeneration, in the hEnMSCs-EXOs group is started faster than those of other groups.

Considering the advantages of the exosome therapeutic strategy, we implemented the conventional method of directed delivery of encapsulated hEnMSCs-EXOs with injection into the myocardium. In this study, we encapsulated hEnMSCs-derived exosomes in fibrin gel before injection to exosomes release gradually and prevent the adverse inflammation during days post MI. Furthermore, we follow up on heart function by echocardiography in 1 and 30 days post-MI. Such kind of treatment may be a more viable therapeutic approach for clinical cardiac regeneration. Although a 30-min interval for door-to-balloon time is too short for clinical application, which is a limitation of this study,

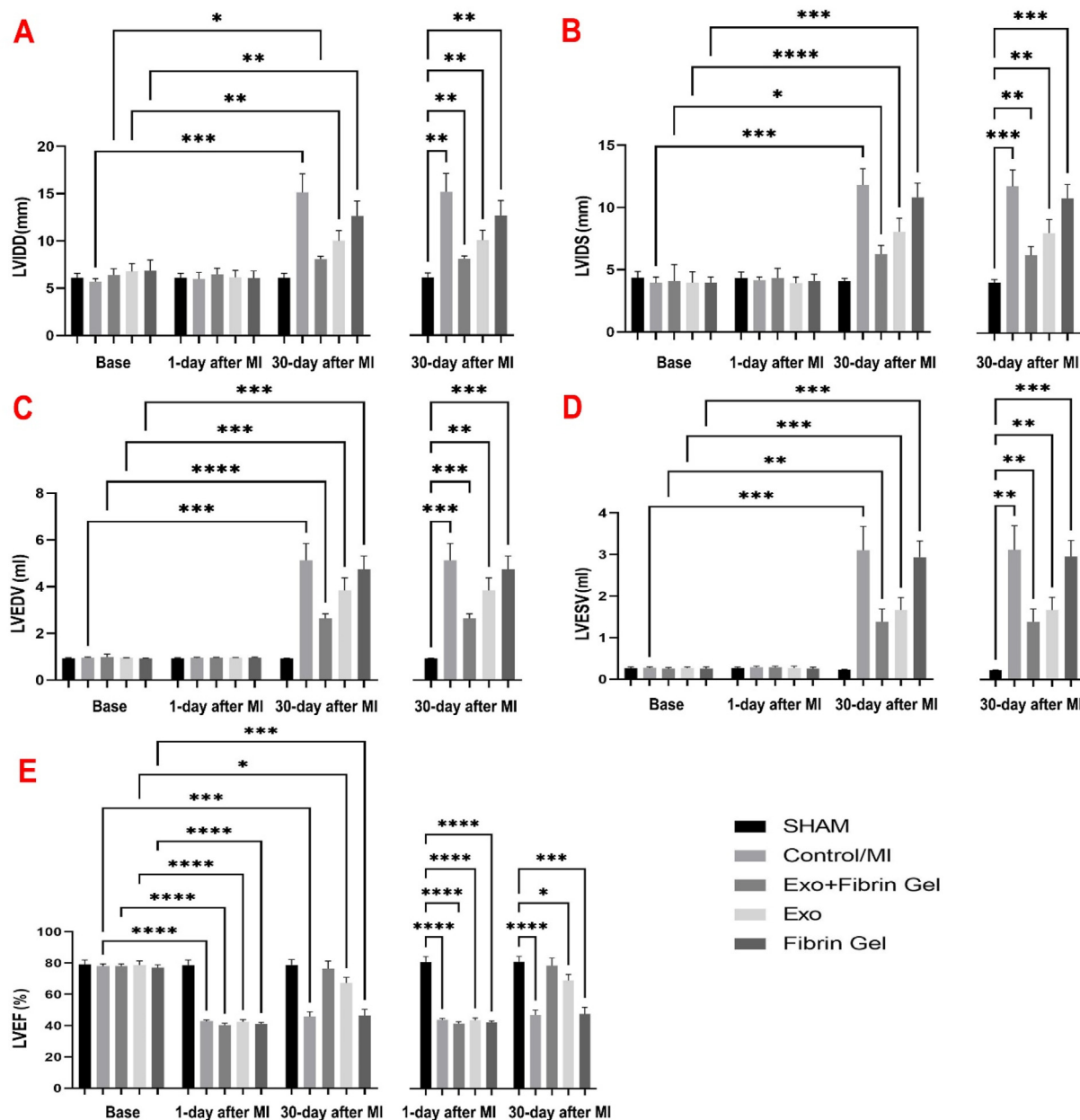


**Fig. 4.** Encapsulated hEnMSCs-EXOs in fibrin gel treatment boosts cardiac functions in a Rat model of MI. (A) Schematic of the study design. Echocardiography post-MI (baseline), 24 h post-MI, and 30 days post-MI (endpoint) (A–E), (n = 5). The parameters include LVDD, LVDS, LVEDV, LVESV, and LVEF. All error bars are presented as mean ± SD. The comparisons between samples were operated by one-way ANOVA, followed by post hoc Bonferroni test. \* Indicates P < 0.05; \*\* indicates P < 0.01; \*\*\* indicates P < 0.001; \*\*\*\* indicates P < 0.0001.

this scheme provides a reference for the design of future large animal experiments and clinical trials. To our knowledge, this is the first known report of an injectable therapy using encapsulated hEnMSCs-EXOs in fibrin gel in the ischemic myocardium to alleviate heart injury due to MI. The results showed a further improved therapeutic efficacy of sequential delivery of hEnMSCs following exosome injection in the rats' MI model and revealed multifaceted mechanisms that enhanced myocardium in the MI area. Moreover, the ratio of cellular degradation, inflammation, and fibrosis decreased and was tolerable for cardiomyocytes to be retained in the ischemic hearts (Fig. 5). Therefore, we reasoned that administration of hEnMSCs-derived exosomes would modulate the ischemic milieu to facilitate angiogenesis and thus could achieve better cardiac repair/regeneration.

#### 4. Conclusion and future perspective

Myocardial infarction (MI) occurs when inadequate oxygen supply to the heart leads to permanent damage to the myocardium tissue. The primary mechanism behind MI-induced damage is ischemic/reperfusion injury (I/R). During ischemia, the lack of oxygen to the affected myocardium causes cell necrosis and death. The limited regenerative ability of cardiomyocytes (CMs) and the formation of fibrotic scar tissue by activated cardiac fibroblasts (CFs) to repair the damaged tissue ultimately results in the loss of heart function and can progress to heart failure. Consequently, significant research is underway to prevent and treat MI. Despite numerous therapeutic strategies, limited success has been achieved due to the heart's restricted self-repair and regenerative capabilities.

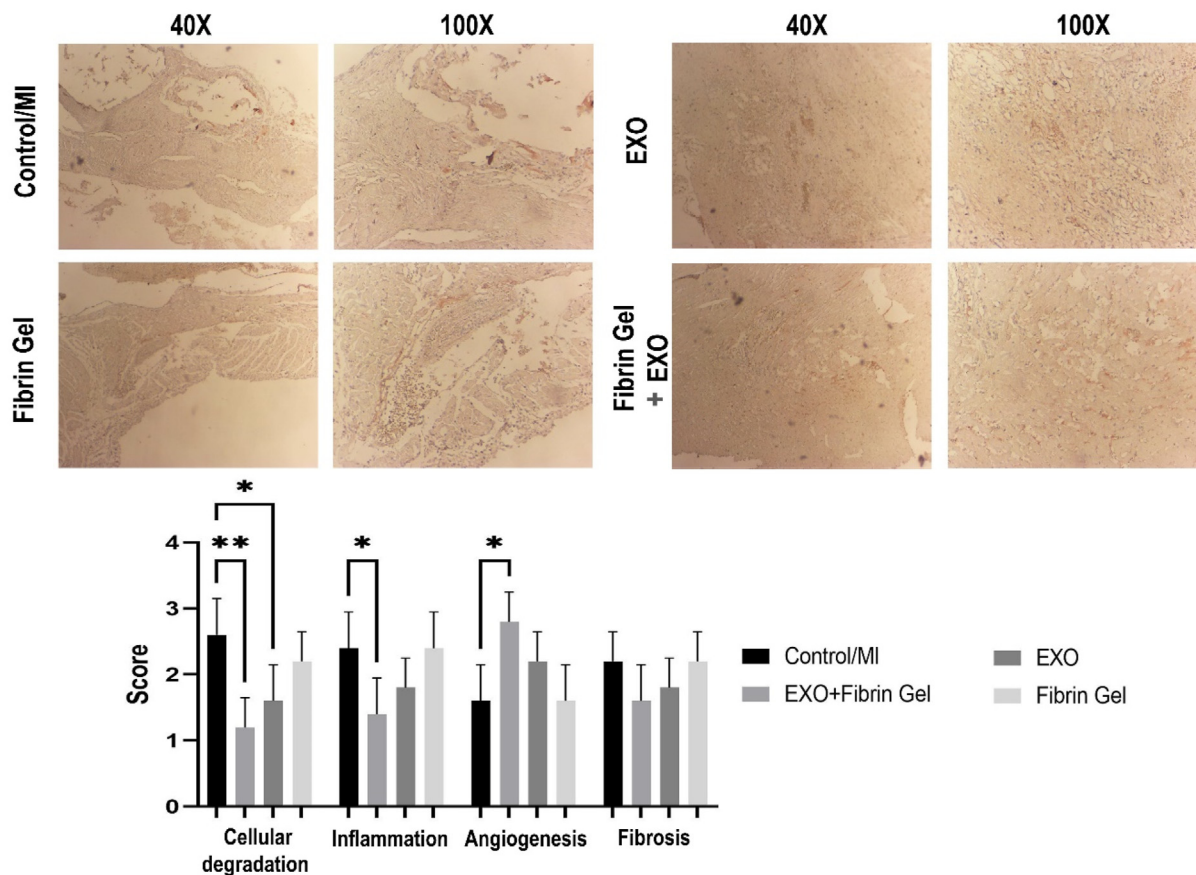


**Fig. 5.** IHC analysis of angiogenesis by monitoring CD31 positive vessels within the infarct border zone 30 days after encapsulated hEnMSCs-EXOs injection. Data indicated the maximum increase of CD31 positive vessels (dark blue points) in the MI injured rat that were injected with encapsulated hEnMSCs-EXOs group compared to the other groups (healthy controls (Sham), MI injury controls, and with fibrin gel, hEnMSCs-EXOs only, fibrin gel only). Moreover, the ratio of cellular degradation, inflammation and fibrosis in the group treated with encapsulated hEnMSCs-EXOs compared to the other groups decreased. Magnifications 40 × and 100 ×. One-way ANOVA with Tukey post hoc analysis. \*p < 0.05; \*\*\*p < 0.001; and \*\*\*\*p < 0.0001.

On the other hand, exosomes have been shown to influence stem cell functions in various ways and enhance tissue repair. In our study, we found that treatment with fibrin gel-encapsulated hEnMSCs-derived exosomes (hEnMSCs-EXOs) significantly improved angiogenesis in the myocardium. Recently, novel approaches, including the use of exosomes, miRNAs, and biomaterials, have been developed to enhance cell-free therapies. We present here the injectable delivery of encapsulated hEnMSCs-EXOs in fibrin gel, which further promotes heart regeneration and function after MI. These advancements highlight the promising potential of exosome therapy. While full myocardial recovery and regeneration remain a goal yet to be achieved in both preclinical and clinical research, ongoing efforts to explore multifaceted cell-free therapeutic strategies such as combining exosomes with biomaterials or integrating them into cardiac patches hold the potential to accelerate progress toward this objective.

**Ethics approval and consent to participate**

All animal experiments were approved by the Ethics Committee of the Tehran University of Medical Sciences (Ethical Approval No. IR. TUMS.AMIRALAM.REC.1402.041) in accordance with institutional and international guidelines.

**Consent for publication**

Not Applicable.

**Availability of data and materials**

The datasets used and analyzed during the current study available from the corresponding author on reasonable request.

**Credit authorship contribution statement**

- Masoumeh Sepehri: Methodology, Investigation, Writing-Original draft.
- Shahram Rabbani: Animal surgery and in vivo animal tests.
- Fatemeh Kouchakzadeh, Mohsen Abedini Esfahlani, Jafar Ai, Hossein Ghanbari: Data analysis.
- Naghme Bahrami: Financial supporting.
- Mojdeh Salehi Namini: exosome isolation.
- Majid Sharifi: Resources and Software.
- Somayeh Ebrahimi-Barough: Supervisions, Conceptualization, Reviewing and Editing.

**Funding**

The authors thank Tehran University of Medical Sciences (Grant No.1402-3-166-68438 and No.1402-2-148-63124) for supporting this research.

**Declaration of competing interest**

The authors clarify that there is no conflict of interests.

## Acknowledgments

The authors thank the Tehran University of Medical Sciences for supporting this research.

## References

- Virani Salim S, Alonso Alvaro, Aparicio Hugo J, Benjamin Emelia J, Bittencourt Marcio S, Callaway Clifton W, et al. Heart disease and stroke statistics. *Circulation* 2021. <https://doi.org/10.1161/CIR.0000000000000950>.
- Cardiovascular diseases (CVDs). Fact sheet. Geneva: World Health Organization; 2021. [https://www.who.int/newsroom/factsheets/detail/cardiovascular-diseases-\[cvds\]](https://www.who.int/newsroom/factsheets/detail/cardiovascular-diseases-[cvds]).
- Doppler Stefanie A, Deutsch Marcus-Andre, Serpooshan Vahid, Li Guang, Dzilic Elda, Lange Rüdiger, et al. Mammalian heart regeneration: the race to the finish line. *Circ Res* 2017. <https://doi.org/10.1161/CIRCRESAHA.116.31005>.
- Laflamme MA, Murry CE. Heart regeneration. *Nature* 2011. <https://doi.org/10.1038/nature10147>.
- Guo Yajun, Yu Yunsheng, Hu Shijun, Chen Yueqiu, Shen Zhenya. The therapeutic potential of mesenchymal stem cells for cardiovascular diseases. *Cell Death Dis* 2020. <https://doi.org/10.1038/s41419-020-2542-9>.
- Clifford David M, Fisher Sheila A, Brunskill Susan J, Doree Carolyn, Mathur Anthony, Watt Suzanne, et al. Stem cell treatment for acute myocardial infarction. *Cochrane Database Syst Rev* 2012. <https://doi.org/10.1002/14651858.CD006536.pub3>.
- Gao Lian R, Chen Yu, Zhang Ning K, Yang Xi L, Liu Hui L, Wang Zhi G, et al. Intracoronary infusion of Wharton's jelly-derived mesenchymal stem cells in acute myocardial infarction: double-blind, randomized controlled trial. *BMC Med* 2015. <https://doi.org/10.1186/s12916-015-0399-z>.
- Lemcke H, Voronina N, Steinhoff G, David R. Recent progress in stem cell modification for cardiac regeneration. *Stem Cell Int* 2018. <https://doi.org/10.1155/2018/1909346>.
- Darzi S, Werkmeister JA, Deane JA, Gargett CE. Identification and characterization of human endometrial mesenchymal stem/stromal cells and their potential for cellular therapy. *Stem Cells Transl Med* 2016. <https://doi.org/10.5966/sctm.2015-0190>.
- Thakur Abhimanyu, Carolina Parra Diana, Motalebnejad Pedram, Brocchi Marcelo, Chen Huanhuan Joyce. Exosomes: small vesicles with big roles in cancer, vaccine development, and therapeutics. *Bioact Mater* 2022. <https://doi.org/10.1016/j.bioactmat.2021.08.029>.
- Khan Kashif, Caron Christophe, Mahmoud Ibtisam, Derish Ida, Schwertani Adel, Cecere Renzo. Extracellular vesicles as a cell-free therapy for cardiac repair: a systematic review and meta-analysis of randomized controlled preclinical trials in animal myocardial infarction models. *Stem Cell Rev Rep* 2022. <https://doi.org/10.1007/s12015-021-10289-6>.
- Alcayaga-Miranda Francisca, Cuenca Jimena, Luz-Crawford Patricia, Aguila-Diaz Carolina, Fernandez Ainoa, Figueroa Fernando E, et al. Characterization of menstrual stem cells: angiogenic effect, migration and hematopoietic stem cell support in comparison with bone marrow mesenchymal stem cells. *Stem Cell Res Ther* 2015. <https://doi.org/10.1186/s13287-015-0013-5>.
- Murphy Michael P, Wang Hao, Patel Amit N, Kambhampati Suman, Niren Angle, Chan Kyle, et al. Allogeneic endometrial regenerative cells: an "Off the shelf solution" for critical limb ischemia? *J Transl Med* 2008. <https://doi.org/10.1186/1479-5876-6-45>.
- Bockeria Leo, Bogin Vladimir, Bockeria Olga, Le Tatyana, Alekyan Bagrat, Woods Erik J, et al. Endometrial regenerative cells for treatment of heart failure: a new stem cell enters the clinic. *J Transl Med* 2013. <https://doi.org/10.1186/1479-5876-11-56>.
- Jiang Zhi, Hu Xinyang, Yu Hong, Xu Yinchuan, Wang Lihan, Chen Han, et al. Human endometrial stem cells confer enhanced myocardial salvage and regeneration by paracrine mechanisms. *J Cell Mol Med* 2013. <https://doi.org/10.1111/jcmm.12100>.
- Tyler J DiStefano, Vaso Ketii, George Danias, Chionuma Henry N, Weiser Jennifer R, Iatridis James C, et al. Extracellular vesicles as an emerging treatment option for intervertebral disc degeneration: therapeutic potential, translational pathways, and regulatory considerations. *Adv Healthcare Mater* 2022. <https://doi.org/10.1002/adhm.202100596>.
- Bei Yihua, Das Saumya, Rodosthenous Rodosthenis S, Holvoet Paul, Vanhaverbeke Maarten, Monteiro Marta Chagas, et al. Extracellular vesicles in cardiovascular theranostics. *Theranostics* 2017. <https://doi.org/10.7150/tno.21274>.
- Song Yaying, Li Zongwei, He Tingting, Qu Meijie, Jiang Lu, Wanlu, et al. M2 microglia-derived exosomes protect the mouse brain from ischemia-reperfusion injury via exosomal mir-124. *Theranostics* 2019. <https://doi.org/10.7150/tno.30879>.
- Xu Meng, Feng Tao, Liu Bowen, Qiu Fen, Xu Youhua, Zhao Yonghua, et al. Engineered exosomes: desirable target-tracking characteristics for cerebrovascular and neurodegenerative disease therapies. *Theranostics* 2021. <https://doi.org/10.7150/tno.62330>.
- Sun S-J, Wei R, Li F, Liao Song-Yan, Hung-Fat Tse. Mesenchymal stromal cell-derived exosomes in cardiac regeneration and repair. *Stem Cell Rep* 2021. <https://doi.org/10.1016/j.stemcr.2021.05.003>.
- Chen Peier, Wang Ling, Fan Xianglin, Ning Xiaodong, Yu Bin, Ou Caiwen, et al. Targeted delivery of extracellular vesicles in heart injury. *Theranostics* 2021. <https://doi.org/10.7150/tno.51571>.
- Thygesen Kristian, Alpert Joseph S, Jaffe Allan S, Chaitman Bernard R, Bax Jeroen J, Morrow David A, et al. Fourth universal definition of myocardial infarction. *Eur Heart J* 2018. <https://doi.org/10.1016/j.jacc.2018.08.1038>.
- Gallet Romain, Dawkins James, Valle Jackelyn, Simsolo Eli, de Couto Geoffrey, Ryan Middleton, et al. Exosomes secreted by cardiosphere-derived cells reduce scarring, attenuate adverse remodeling, and improve function in acute and chronic porcine myocardial infarction. *Eur Heart J* 2017. <https://doi.org/10.1093/eurheartj/ehw240>.
- Contessotto P, Pandit A. Therapies to prevent post-infarction remodeling: from repair to regeneration. *Biomaterials* 2021. <https://doi.org/10.1016/j.biomaterials.2021.120906>.
- Hockel M, Schlenger K, Doctrow S, Kissel T, Vaupal P. Therapeutic angiogenesis. *Arch Surg* 1993. <https://doi.org/10.1177/1358863X960010011>.
- Bian Suyan, Zhang Liping, Duan Liufa, Wang Xi, Min Ying, Yu Hepeng. Extracellular vesicles derived from human bone marrow mesenchymal stem cells promote angiogenesis in a rat myocardial infarction model. *J Mol Med (Berl)* 2014. <https://doi.org/10.1007/s00109-013-1110-5>.
- Xin Hongqi, Li Yi, Cui Yisheng, Yang James J, Zhang Zheng Gang, Chopp Michael. Systemic administration of exosomes released from mesenchymal stromal cells promote functional recovery and neurovascular plasticity after stroke in rats. *J Cerebr Blood Flow Metabol* 2013. <https://doi.org/10.1038/jcbfm.2013.152>.
- Zhang Jiyeuan, Guan Junjie, Niu Xin, Hu Guowen, Guo Shangchun, Li Qing, Xie Zongping. Exosomes released from human induced pluripotent stem cell-derived MSCs facilitate cutaneous wound healing by promoting collagen synthesis and angiogenesis. *J Transl Med* 2015. <https://doi.org/10.1186/s12967-015-0417-0>.
- Sanganalmath SK, Bolli R. Cell therapy for heart failure: a comprehensive overview of experimental and clinical studies, current challenges, and future directions. *Circ Res* 2013. <https://doi.org/10.1161/CIRCRESAHA.113.300219>.
- Singla DK. Stem cells and exosomes in cardiac repair. *Curr Opin Pharmacol* 2016. <https://doi.org/10.1016/j.coph.2016.01.003>.
- Wernly Bernhard, Mirna Moritz, Rezar Richard, Proding Christine, Jung Christian, Podesser Bruno K, et al. Regenerative cardiovascular therapies: stem cells and beyond. *Int J Mol Sci* 2019. <https://doi.org/10.3390/ijms20061420>.
- Ratajczak MZ, Kucia M, Jadczyk T, Greco NJ, Wojakowski W, Tendera M, et al. Pivotal role of paracrine effects in stem cell therapies in regenerative medicine: can we translate stem cell-secreted paracrine factors and microvesicles into better therapeutic strategies? *Leukemia* 2012. <https://doi.org/10.1038/leu.2011.389>.
- Balalubramanian P, Prabhakaran MP, Kai D, Ramakrishna S. Human cardiomyocyte interaction with electrospun fibrinogen/gelatin nanofibers for myocardial regeneration. *J Biomater Sci Polym* 2013. <https://doi.org/10.1080/09205063.2013.789958>.
- Ravichandran Rajeswari, Reddy Venugopal Jayarama, Subramanian Sundarajan, Mukherjee Shayanti, Sridhar Radhakrishnan, Ramakrishna Seeram. Expression of cardiac proteins in neonatal cardiomyocytes on PGS/fibrinogen core/shell substrate for Cardiac tissue engineering. *Int J Cardiol* 2013. <https://doi.org/10.1016/j.ijcard.2012.04.045>.
- National Institutes of Health (NIH). National research council (US) committee for the update of the guide for the care and use of laboratory animals. Washington (DC): National Academies Press (US); 2011. <https://doi.org/10.17226/12910>.
- Mohamadi Forouzan, Ebrahimi-Barough Somayeh, Reza Nourani Mohammad, Mansoori Korosh, Salehi Majid, Ali Akbar Alizadeh, et al. Enhanced sciatic nerve regeneration by human endometrial stem cells in an electrospun poly( $\epsilon$ -caprolactone)/collagen/NBC nerve conduit in rat. *Artif Cells, Nanomed Biotechnol* 2018. <https://doi.org/10.1080/21691401.2017.1391823>.
- Rannou Alice, Toumaniantz Gilles, Larcher Thibaut, Leroux Isabelle, Ledevin Mireille, Hivonnait Agnès, et al. Human MuStem cell grafting into infarcted rat heart attenuates adverse tissue remodeling and preserves cardiac function. *Mol Ther: Methods Clinical Development* 2020. <https://doi.org/10.1016/j.omtm.2020.06.009>.
- Takagawa Junya, Zhang Yan, Wong Maelene L, Sievers Richard E, Kapasi Neel K, Wang Yan, et al. Myocardial infarct size measurement in the mouse chronic infarction model: comparison of area- and length-based approaches. *J Appl Physiol* 2007. <https://doi.org/10.1152/jappphysiol.00033.2007>.
- Taghdiri Nooshabadi Vajihe, Khanmohammadi Mehdi, Shafei Shilan, Banafshe Hamid Reza, Veisi Malekshahi Ziba, Ebrahimi-Barough Somayeh, et al. Impact of atorvastatin loaded exosome as an anti-glioblastoma carrier to induce apoptosis of U87 cancer cells in 3D culture model. *Biochemistry Biophysics Reports* 2020. <https://doi.org/10.1016/j.bbrep.2020.100792>.
- Hu Guo-wen, Li Qing, Niu Xin, Hu Bin, Liu Juan, Zhou Shu-min, et al. Exosomes secreted by human-induced pluripotent stem cell-derived mesenchymal stem cells attenuate limb ischemia by promoting angiogenesis in mice. *Stem Cell Res Ther* 2015. <https://doi.org/10.1186/s12875-015-0546-6>.
- Tompkins Bryon A, Balkan Wayne, Winkler Johannes, Gyöngyösi Mariann, Gollasch Georg, Fernández-Avilés Francisco, et al. Preclinical studies of stem cell therapy for heart disease. *Circ Res* 2018. <https://doi.org/10.1161/CIRCRESAHA.117.312486>.

- [42] Pavo Noemi, Charwat Silvia, Nyolczas Noemi, Jakab András, Murlasits Zsolt, Bergler-Klein Jutta, et al. Cell therapy for human ischemic heart diseases: critical review and summary of the clinical experiences. *J Mol Cell Cardiol* 2014. <https://doi.org/10.1016/j.yjmcc.2014.06.016>.
- [43] Huang P, Tian X, Li Q, Yang Y. New strategies for improving stem cell therapy in ischemic heart disease. *Heart Fail Rev* 2016. <https://doi.org/10.1007/s10741-016-9576-1>.
- [44] Poe AJ, Knowlton AA. Exosomes as agents of change in the cardiovascular system. *J Mol Cell Cardiol* 2017. <https://doi.org/10.1016/j.yjmcc.2017.08.002>.
- [45] Ong Sang-Ging, Lee Won Hee, Huang Mei, Dey Devaveena, Kodo Kazuki, Sanchez-Freire Veronica, et al. Cross talk of combined gene and cell therapy in ischemic heart disease: role of exosomal microRNA transfer. *Circulation* 2014. <https://doi.org/10.1161/CIRCULATIONAHA.113.007917>.
- [46] Yu B, Kim HW, Gong M, Wang J, Millard RW, Wang Y, et al. Exosomes secreted from GATA-4 overexpressing mesenchymal stem cells serve as a reservoir of anti-apoptotic microRNAs for cardioprotection. *Int J Cardiol* 2015. <https://doi.org/10.1016/j.ijcard.2014.12.043>.